Multianalytical Study of Patina Formed on Archaeological Metal Objects from Bliesbruck-Reinheim

Michael Wadsak[1,*]**, Ina Constantinides**[3]**, Guido Vittiglio**[3]**, Annemie Adriaens**[3]**, Koen Janssens**[3]**, Manfred Schreiner**[1,2]**, Freddy C. Adams**[3]**, Philippe Brunella**[4]**,** and **Michel Wuttmann**[5]

[1] Institute of Analytical Chemistry, Vienna University of Technology, Getreidemarkt 9/151, A-1060 Vienna, Austria
[2] Institute of Chemistry, Academy of Fine Arts, Schillerplatz 3, A-1010 Vienna, Austria
[3] Micro and Trace Analysis Center (MiTAC), Dept. of Chemistry, University of Antwerp, Universiteitsplein 1, 2610 Wilrijk, Belgium
[4] Centre Archéologique Départemental, Bliesbruck, France
[5] Institut Français d'Archéologie Orientale, Rue el-Cheikh Ali Youssef 37, B.P. Qasr al-Aïny 11562 Cairo, Egypt

Abstract. Patinas naturally formed on archaeological bronze alloys were characterized using light microscopy (LM), micro energy dispersive X-ray fluorescence analysis (μ-EDXRF), time of flight secondary ion mass spectrometry (TOF-SIMS) and scanning electron microscopy in combination with energy dispersive X-ray microanalysis (SEM/EDX). The examinations carried out on cross-sections of samples have shown that in all samples the copper content in the corrosion layer is lower than in the bulk, while an increase of tin and lead could be observed. Two different types of corrosion were found: first type, a corrosion formation leading to a three layer structure was observed on lead bronze. The outer layer consists mainly of Cu(II) compounds and soil material, followed by a fragmented layer of cuprous oxide and the surface layer of the alloy, where a depletion of copper and an enrichment of tin and high amounts of Cl could be detected. The second type of corrosion is characterized by a two layer structure on the tin bronze sample consisting of an outer layer with copper containing corrosion products and a layer with cracks, which reveals a depletion of copper whereas tin and lead are enriched. Also high amounts of Si were detected in this surface layer.

Key words: Archaeometry; microanalysis; copper alloys; corrosion.

When exposed to the ambient atmosphere, copper and copper alloys form a thin layer of corrosion. This layer is called patina and appears to be generally brownish-green or greenish-blue. Patinas are chemically and metallurgically complex structures. A large number of studies on ancient and historical bronzes have tried to establish the chemical characteristics and structure of natural patinas grown on artifacts exposed to soil [1–3] or the ambient atmosphere [4–7] for a long time. Archaeological artifacts represent excellent samples for such studies as they are of great importance for scientists and conservators to control and stop the process of deterioration of ancient and historic metals in museums.

Previous investigations concerning the classical structure of corrosion products of copper alloys by Organ [8] reveal that the main constituents of the surface layer of the patina are green coloured copper(II) compounds covering a red cuprous oxide layer in contact with the metal core of the alloy. Depending on the environment these copper(II) salts are malachite $Cu_2(CO_3)(OH)_2$ formed in soil, brochantite $CuSO_4 \cdot 3Cu(OH)_3$ in the atmosphere and atacamite $CuCl_2 \cdot 3Cu(OH)_2$ in the seawater. It is also well known that tin is selectively dissolved from the alloy into the outer medium which is referred as destanification or tin de-alloying [1, 9].

The present work is part of the IMMACO-Project (Improvement of Means of Measurement on Archaeological Copper Alloys for Characterization and

---

* To whom correspondence should be addressed

Conservation) within the frame of the Standards, Measurements and Testing (SMT) Programme of the European Union, DG XII, and aims the development of reliable tools for archaeometers and researchers in the field of conservation. Within the scope of this paper light microscopy (LM), micro energy dispersive X-ray fluorescence analysis (μ-EDXRF), time of flight secondary ion mass spectrometry (TOF-SIMS) and energy dispersive X-ray microanalysis in a scanning electron microscope (SEM/EDX) are applied to analyze the corrosion structures on various interfaces between metal and the corrosion products with emphasis on the layer composition, layer structure, presence or lack of soil elements and nature of the corrosion layers. Two fragments of archaeological metal objects were selected for the present study from a group of 50 objects excavated at the archaeological site of Bliesbruck-Reinheim (on the border between Germany and France). This is the site of a Roman town situated at the northern boundary of the Roman Empire on the Blies river during the 1st century AD. In the urban area several districts have been identified. The end of the site occupation is attested to the end of the 5th century [10–12]. Tin and lead bronzes are predominantly excavated. In some cases also quaternary bronzes and brass were found. Both samples investigated show a heterogeneous microstructure characterized by various inclusions of copper oxide, copper or lead sulfide. The elementary composition was determined by SEM/EDX on polished cross sections. The first fragment is a lead bronze (excavation No. 91.963) and is a piece of solidificated bronze waste. The second one is a tin bronze (excavation No. 91.911c) and is described as a bottom from a beaker.

Experimental

In this study a set of different analytical techniques has been applied in combination since each method provides specific information about the structure of the corrosion layers and the bulk of the metal. Light microscopy was used to obtain a rapid and representative characterization of the microstructure in terms of the classical metallographic description of an alloy. Information on the size of the phases and their distribution across mm-domains were achieved from large and representative areas of the specimens. μ-EDXRF was used to perform quantitative investigations of the bulk and the corroded surface region. The application of this technique is preferred to conventional XRF in archaeometry due to the fact that the latter method is severely hampered by the large size of the irradiated area (at least 1 cm^2) preventing details of decorations, shapes etc. to be analyzed separately. Also the irradiation geometry and sample surface are usually non-ideal and
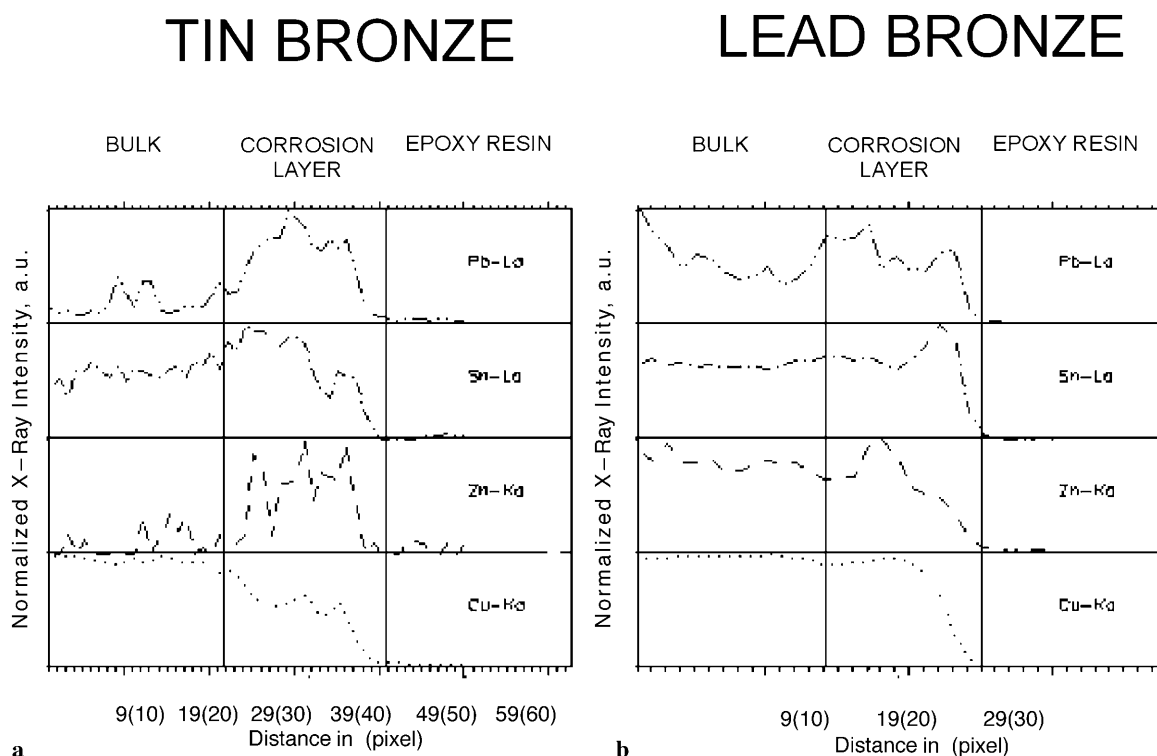

Fig. 1. μ-EDXRF line scans for Pb, Sn, Zn and Cu for an archaeological tin bronze (a) and a lead bronze artifact (b). The scans were performed on cross-sectioned samples from the bulk (left) through the corrosion layer (center) into the epoxy resin

not well defined possibly causing systematic errors in the quantification. Additionally, line scans from the bulk into the corrosion layer were recorded on cross-sections with μ-EDXRF to show differences in the composition. The characterization of the corrosion layer was carried out by using backscattered electron images (BE) and elemental distributions (X-ray mappings) with energy dispersive X-ray microanalysis in a scanning electron microscope (SEM/EDX). For these investigations a Jeol JSM 6400 instrument in combination with an energy dispersive X-ray microanalysis system, Link eXL, was used. Furthermore, time of flight secondary ion mass spectrometry (TOF-SIMS) was applied to obtain additional information on matrix and trace elements. A TOF-SIMS IV Cameca instrument equipped with a Ga^+ liquid metal ion source was available therefore.

The samples were cross-sectioned, embedded in epoxy resin and polished with SiC paper of mesh 600–4000 (grain size 30–5 μm). For the SEM/EDX investigations the samples had to be coated with a thin carbon layer prior to analysis in order to avoid any charging effects.

Results and Discussion

Figure 1 shows μ-EDXRF line scans across the two samples, the tin bronze and the lead bronze. Results clearly indicate that the copper content in the corrosion layer has decreased to 55% in comparison to the bulk for the tin bronze and to 62% for the lead bronze, while the Zn concentration remains constant. Tin and lead have dramatically increased in the corrosion layer. The amount of tin is twice as high as in the bulk of the tin bronze and for the lead bronze the concentration has increased to a value three times higher. Also a drastic increase of lead in the corrosion zone can be observed. The line scans with XRF shown in Fig. 1 underline the changes in composition from the bulk into the corrosion layer of the two alloys. It

can be clearly seen for both alloys that the copper content decreases in the corrosion zone whereas the amount of Sn increases. The enrichment of Zn in the corrosion layer can be explained by the rather low
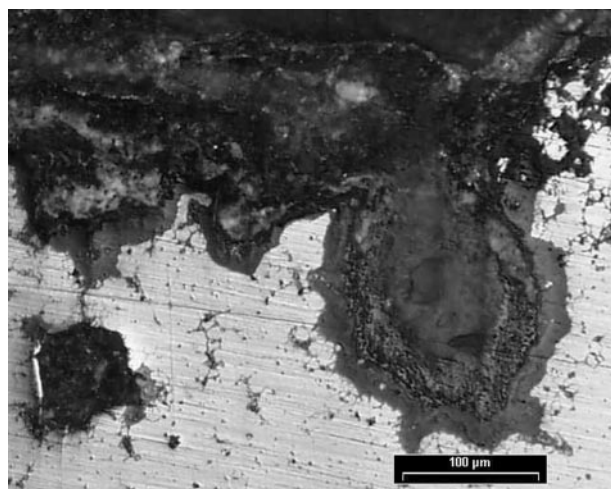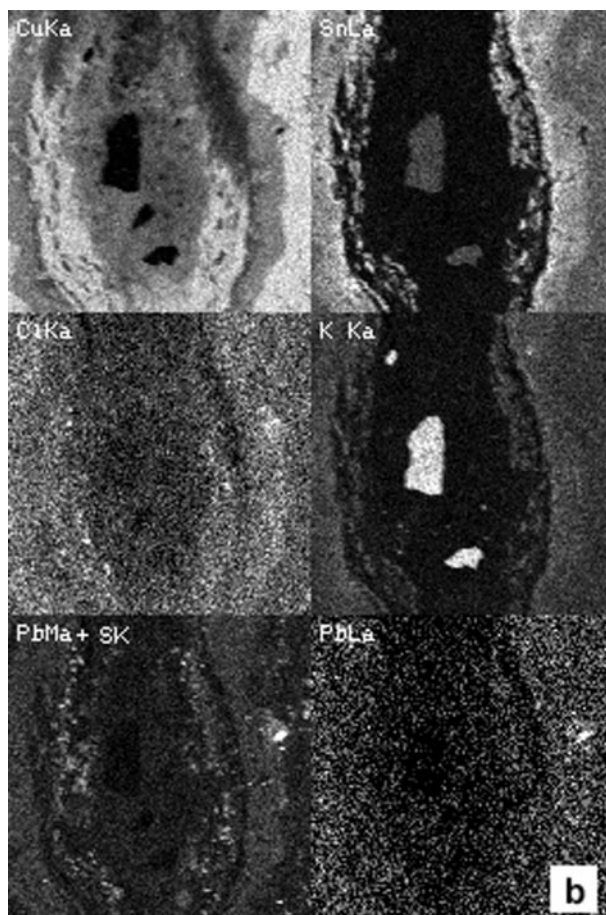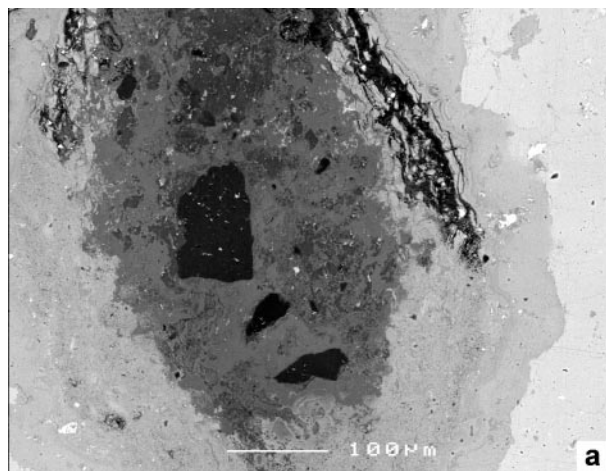

Fig. 3. Backscattered electron image (*BE*) of a cross-section of the lead bronze (a) with the corresponding elemental distribution of Cu, Sn, Cl, K, S K + Pb Mα and Pb Lα (b)

Fig. 2. Light microscopy image of the cross-section of the lead bronze. Various layers are clearly visible

concentration in the bulk. Also the higher amounts of lead in the corrosion layer compared to the bulk can be clearly seen. The high concentration of lead in the bulk of the lead bronze at the beginning of the scan in Fig. 1b is obviously caused by microheterogeneities.

Optical examinations of the cross-section of the lead bronze reveal a heterogeneous structure of the corrosion layer (Fig. 2). The corrosion layer is approximately 150 μm thick and covers the original surface. In some areas, however, the corrosion process has destroyed the original surface leading to loss of matter. Three layers are recognizable within the corrosion, which differ in composition clearly visible in the backscattered electron image (Fig. 3a). The external zone consists of green Cu(II) compounds. X-ray mapping (Fig. 3b) and TOF-SIMS mapping (Fig. 4b) reveal that also K, Si and Al can be found in this layer which is assigned to soil material. The S K-
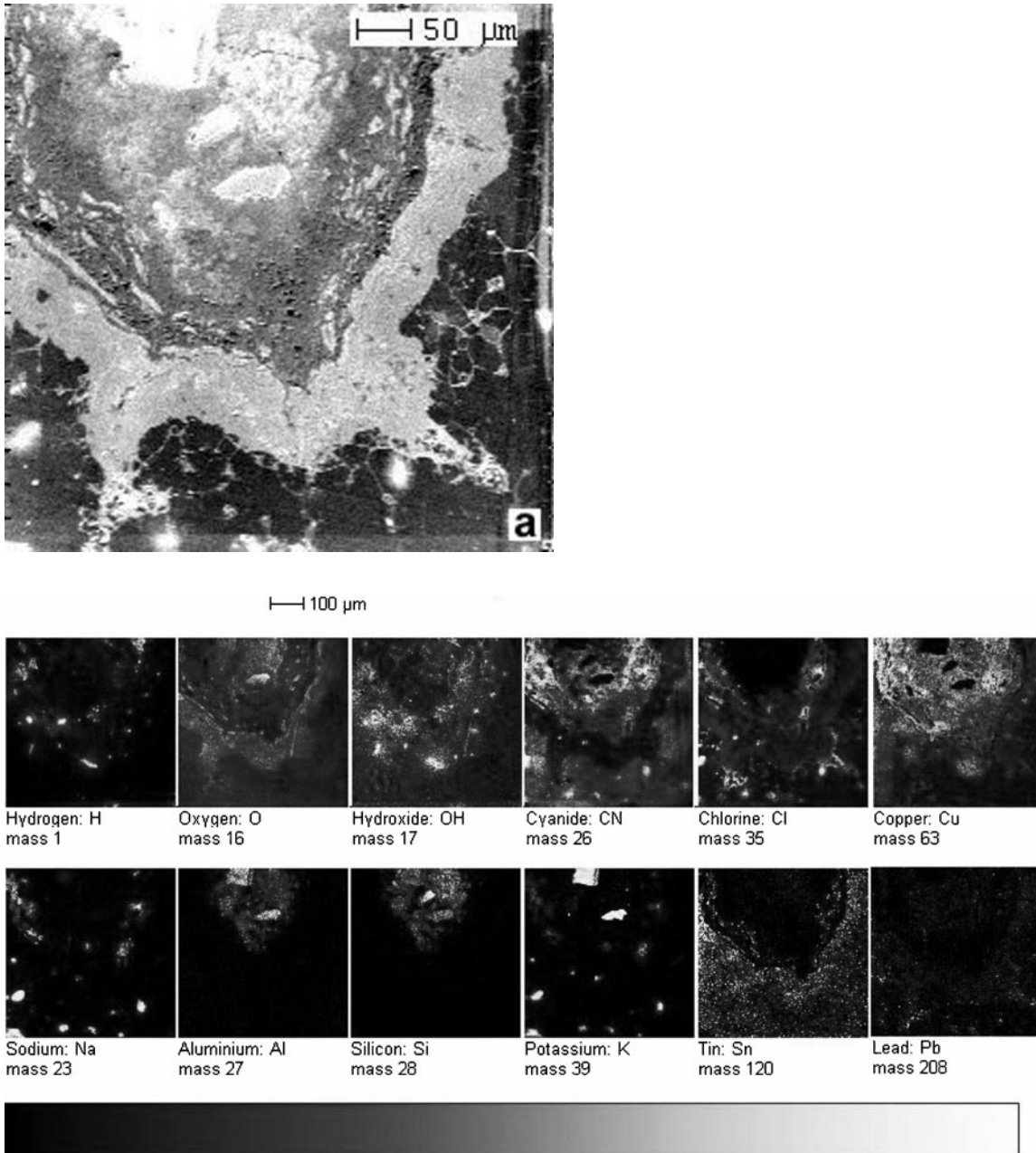

Fig. 4. Secondary electron (a) image (*SE*) and corresponding TOF-SIMS mapping (b) of the cross-sectioned corrosion zone of the lead bronze. The scanned area is 500 μm × 500 μm

lines, which have a coincidence with the Pb Mα-lines, are also present in the corrosion products. Also CN is found, which is shown in the mapping in Fig. 4. This l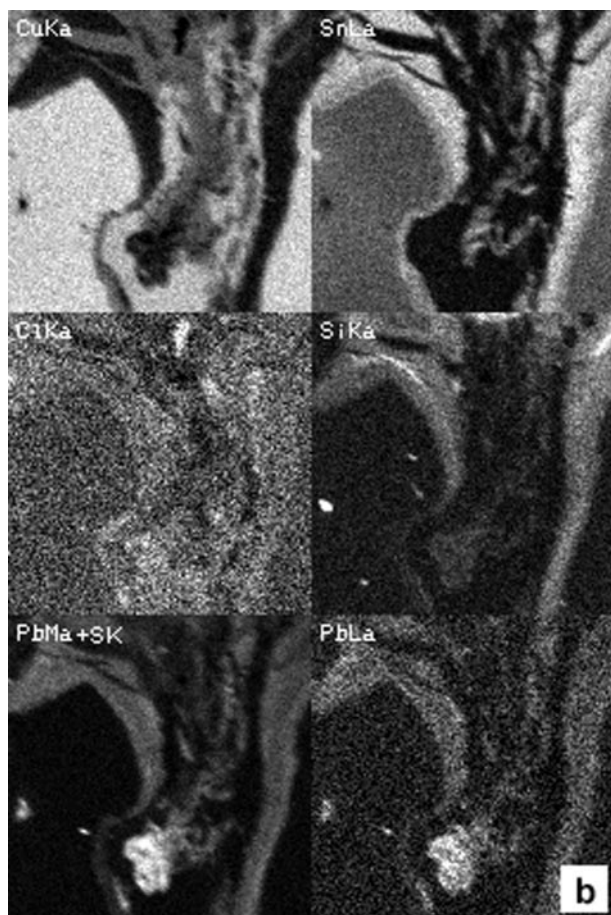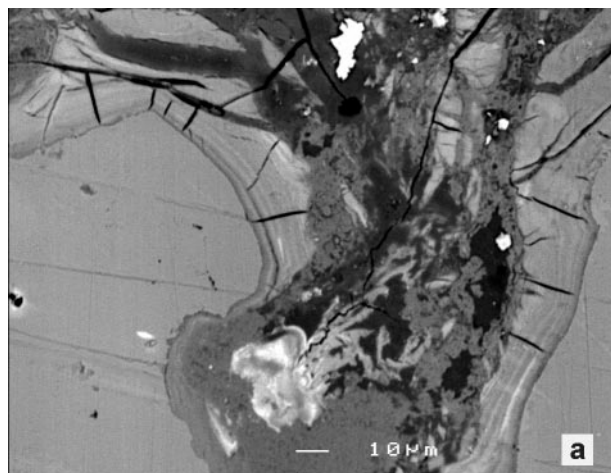ayer is followed by a fragmented red layer of cuprous oxide. This region shows a higher copper content than the prior mentioned and also some tin is present. The internal layer in contact with the alloy consists of brown and orange corrosion products. The elemental distribution (Fig. 3b) shows a depletion of copper and an enrichment of tin in this layer. A high amount of Cl is detected with SEM/EDX at the layer/alloy interface and also oxygen with TOF-SIMS in this area. This layer is considered to be some kind of "ghost" microstructure of the original surface of the alloy described in the literature [3].

In contrast to the results of the lead bronze investigations, the tin bronze sample reveals a different structure of the corrosion layers. From the BE image (Fig. 5a) two corrosion layers can be observed, an outer layer consisting of copper containing corrosion products and an inner layer in contact with the alloy. Big cracks reaching from the inner/ outer layer interface through the layer to the inner layer/alloy interface are clearly visible. The elemental distribution (Fig. 5b) shows a depletion of copper in the inner layer whereas tin is enriched. Considering the coincidence of the S K-lines with the Pb Mα-lines and comparing their X-ray intensities in the X-ray mappings it can be followed that an enrichment of lead is detected in the inner corrosion layer. However, some lead is also found in the corrosion products, where it is not distributed as homogeneous as in the inner layer. Si is not only found in the corrosion products, but also high amounts are detected in the inner layer.

Fig. 5. Backscattered electron image (*BE*) of a cross-section of the tin bronze (a) with the corresponding elemental distribution of Cu, Sn, Cl, Si, S K + Pb Mα and Pb Lα (b)

Conclusion

The investigations carried out on different archaeological bronze artifacts have shown that the combination of light microscopy, micro energy dispersive X-ray fluorescence analysis, time of flight secondary ion mass spectrometry and energy dispersive X-ray microanalysis in a scanning electron microscope is well suitable for the characterization of the corrosion phenomena formed during centuries on the surfaces of such objects. In accordance to the classification of natural patinas on archaeological bronzes (Cu-Sn alloys) two different types of corrosion were observed: a three layer corrosion structure on the lead bronze, which is in good accordance to the Type II or "coarse" surface described by Robbiola et al. [3], and a two layer structure on the tin bronze, similar to the Type I or "even" surface. However, differences

in the composition of the layers and in the presence of cracks were observed. The presence of CN in the tin bronze is an unexpected result and should be examined more in detail. It must be assumed that this result is not an artifact of sample preparation or contamination as all samples from Bliesbruck have been only cleaned from their earth crust and no chemical treatment has been applied.

References

[1] W. Geilmann, *Angew. Chem.* **1956**, *68,* 201.

[2] L. Robbiola, L. P. Hurtel, *Standard Nature of the Passive Layers of Buried Archaeological Bronze*, METAL 95, International Conference on Metals Conservation. James & James Ltd., London, 1997, p. 109.

[3] L. Robbiola, J.-M. Blengino, C. Fiaud, *Corros. Sci.* **1998**, *40,* 2083.

[4] T. E. Graedel, *Corros. Sci.* **1987**, *27,* 639, 721, 741.

[5] B. Pichler, A. Vendl, *Restauratorenblätter* **1990**, *11,* 34.

[6] K. P. Fitzgerald, J. Nairn, A. Atrens, *Corros. Sci.* **1998**, *40,* 2029.

[7] M. Schreiner, G. Woisetschläger, I. Schmitz, M. Wadsak, *J. Anal. At. Spectrom.* **1999**, *14,* 395.

[8] R. M. Organ, *Studies in Conservation* **1963**, *8,* 1.

[9] R. T. Tylecote, *J. Archaeological Science* **1979**, *6,* 345.

[10] H. Boecking, Ph. Brunella, S. Erbelding, N. Legendre, A. Miron, F. Mueller, J-P. Petit, W. Reinhard, J. Schaub, *IMMACO Work Package, no. 1*. Rapport Provisoire, Stiftung Europaeischer Kulturpark Bliesbruck-Reinheim (S.E.K.) IMMACO EEC Programme (contract no. SMT4CT96-2055), Antwerp, 1997, p. 29.

[11] N. Lacoudre, T. Beldjoudi, S. Andrieu, *IMMACO Work Package, no. 1*. Rapport Final, EDF-VALECTRA no. RX971602/2. IMMACO EEC Programme (contract no. SMT4CT96-2055), Antwerp, 1997, p. 67.

[12] J.-P. Petit, M. Mangin, Ph. Brunella (Eds.) Actes du Colloque "Les agglomérations secondaires de Gaule Belgique et des Germanies", Bliesbruck-Blitche, Oct. 1992. Editions Errance, 1994.